# Supporting Information

## Template-Free, Self-doped Approach to Porous Carbon Spheres with High N/O Contents for High-Performance Supercapacitors

Danfeng Xue,[†] Dazhang Zhu,[†] Wei Xiong,[‡] Tongcheng Cao,[†,⊥] Zhiwei Wang,[§] Yaokang Lv,[¶] Liangchun Li,[†] Mingxian Liu,*[,†,§] Lihua Gan*[,†]

[†]Shanghai Key Lab of Chemical Assessment and Sustainability, School of Chemical Science and Engineering, Tongji University, 1239 Siping Road, Shanghai 200092, P. R. China

[‡]Key Laboratory for Green Chemical Process Ministry of Education, School of Chemistry and Environmental Engineering, Wuhan Institute of Technology, 693 Xiongchu Road, Wuhan 430073, P. R. China

[§]State Key Laboratory of Pollution Control and Resources Reuse, Shanghai Institute of Pollution Control and Ecological Security, College of Environmental Science and Engineering, Tongji University, 1239 Siping Road, Shanghai 200092, P. R. China

[¶]College of Chemical Engineering, Zhejiang University of Technology, 18 Chaowang Road, Hangzhou 310014, P. R. China

[⊥]Key Laboratory of Road and Traffic Engineering of Ministry of Education, Tongji University, 4800 Caoan Road, Shanghai 201804, P. R. China

*E-mail: liumx@tongji.edu.cn (M. L.),

* E-mail: ganlh@tongji.edu.cn (L. G.)

The supporting information contains 10 pages, 6 Figures and 4 Tables.

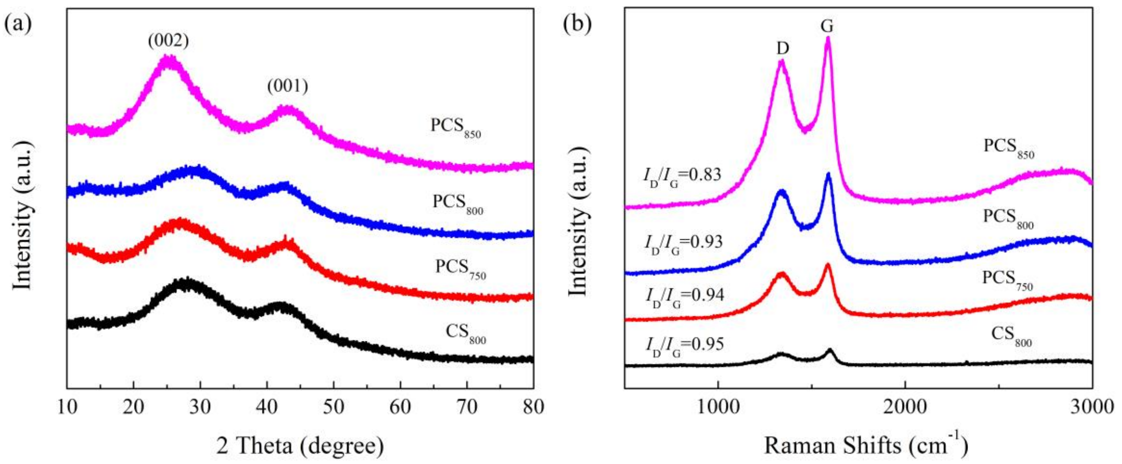


**Figure S1.** XRD patterns (a) and Raman spectra (b) of $CS_{800}$ and PCSs.

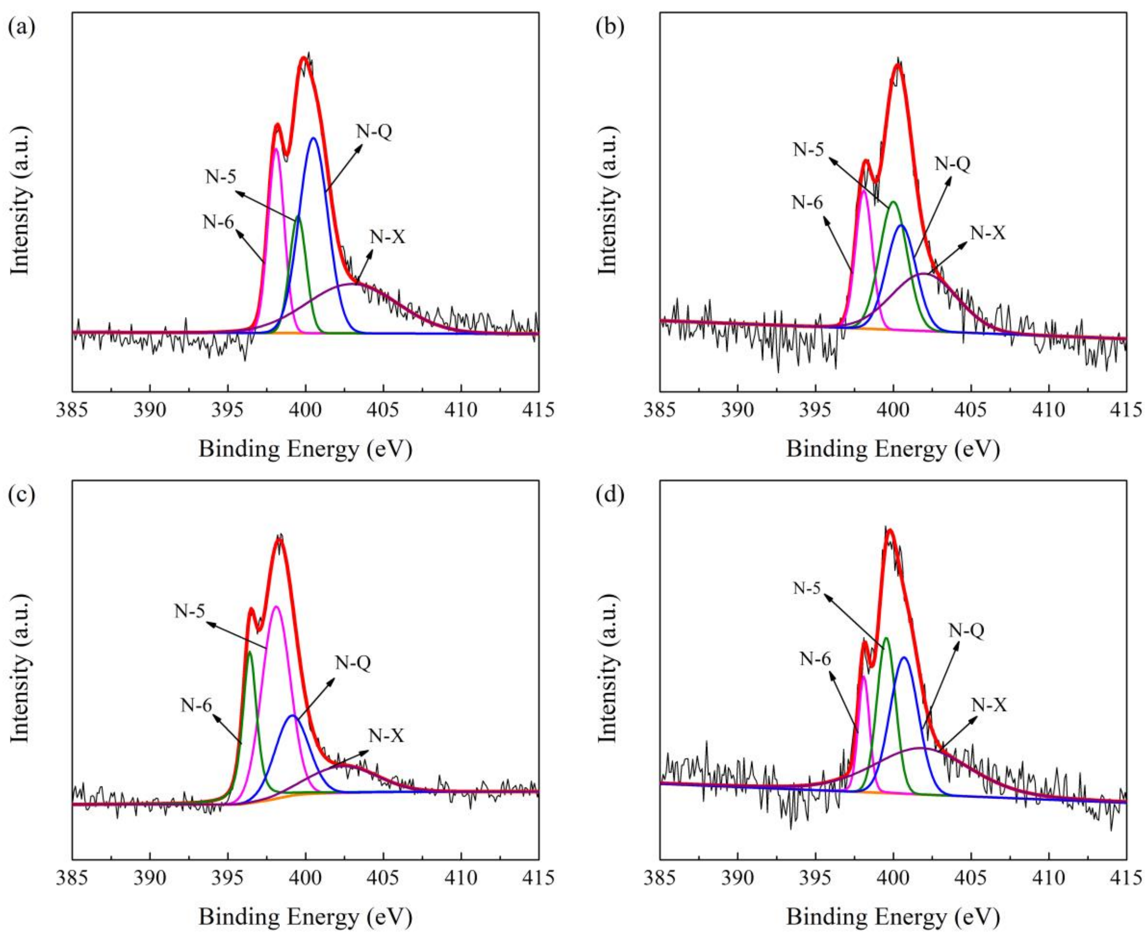


**Figure S2.** N1s high-resolution spectra of $CS_{800}$ (a), $PCS_{750}$ (b), $PCS_{800}$ (c) and $PCS_{850}$ (d).

**Table S1.** Summary of XPS analysis of PCSs.

| Samples | The relative intensity of the dopant species (%) | | | |
|---|---|---|---|---|
| | N-6 | N-5 | N-Q | N-X |
| $CS_{800}$ | 21.5 | 15.7 | 48.1 | 14.7 |
| $PCS_{750}$ | 34.7 | 31.7 | 21.8 | 11.8 |
| $PCS_{800}$ | 30.9 | 41.0 | 13.3 | 14.8 |
| $PCS_{850}$ | 14.4 | 34.2 | 25.2 | 26.2 |

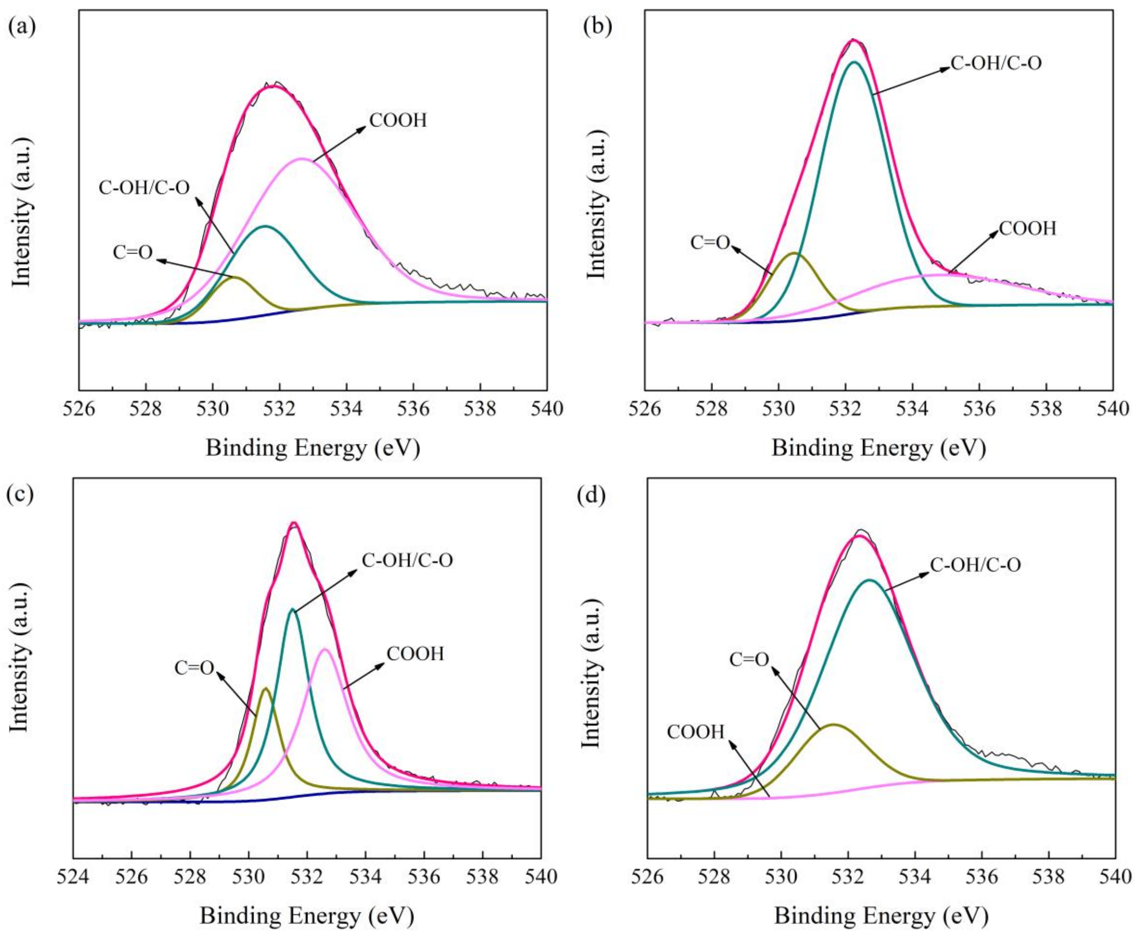


**Figure S3**. O1s high-resolution spectra of $CS_{800}$ (a), $PCS_{750}$ (b), $PCS_{800}$ (c) and $PCS_{850}$ (d).

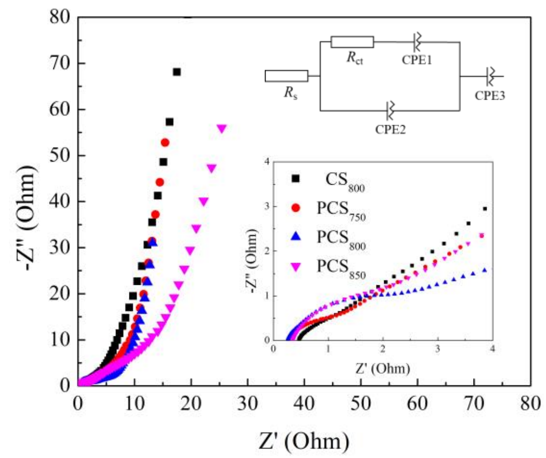


**Figure S4.** The equivalent circuit model of electrode, Nyquist plots of $CS_{800}$ and PCSs electrodes in 6 M KOH electrolyte.

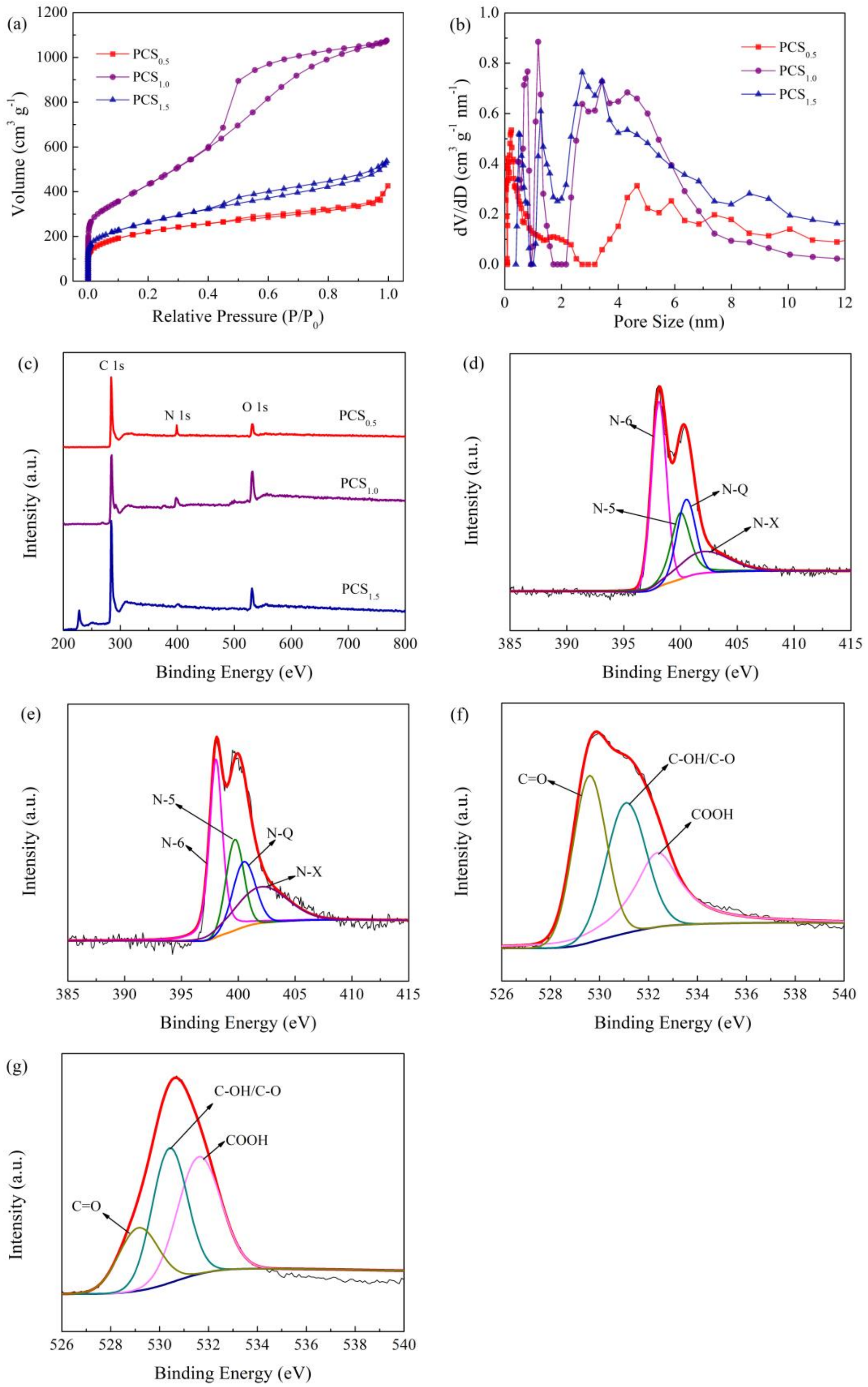


**Figure S5.** Nitrogen sorption isotherms (a), and the curves of pore size distribution (b) of PCSs. Wide-scan XPS data of PCSs (c). N1s and O1s high-resolution spectra of PCSs (d–g).

**Table S2.** Porosity Parameters and Surface Element Contents of PCSs. [a]

| Samples | $S_{BET}$ ($m^2$ $g^{-1}$) | $S_{micro}$ ($m^2$ $g^{-1}$) | $S_{meso}$ ($m^2$ $g^{-1}$) | $V_{total}$ ($cm^3$ $g^{-1}$) | C (wt %) | N (wt %) | O (wt %) |
|---|---|---|---|---|---|---|---|
| $PCS_{0.5}$ | 657 | 404 | 253 | 0.97 | 83.16 | 9.11 | 7.73 |
| $PCS_{1.0}$ | 1321 | 680 | 641 | 1.66 | 82.88 | 7.97 | 10.16 |
| $PCS_{1.5}$ | 768 | 406 | 362 | 0.77 | 88.9 | 2.45 | 8.65 |

[a] $S_{BET}$, $S_{micro}$ and $S_{meso}$, specific surface area, micropore surface area and mesopore surface area; $V_{total}$, the total pore volume.

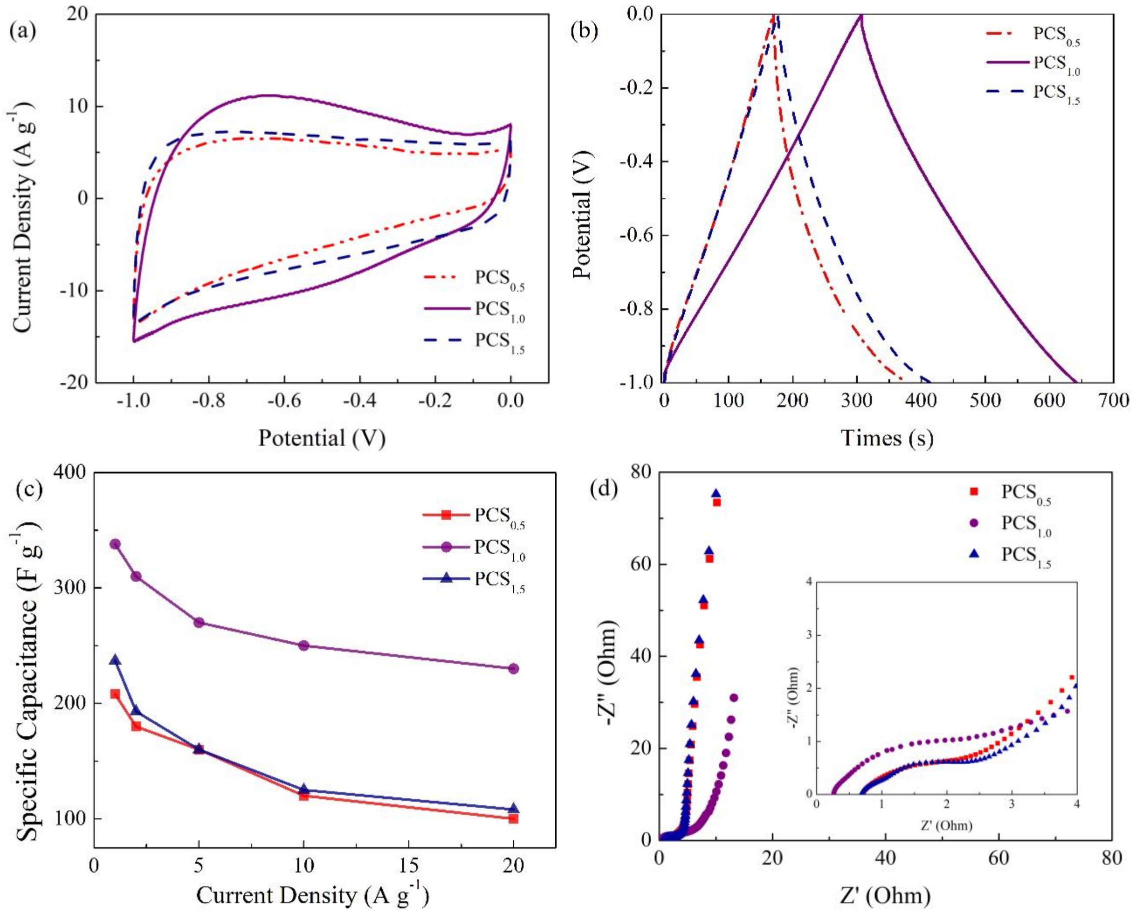


**Figure S6.** CV curves of PCSs electrodes at 50 mV $s^{-1}$ (a), GCD curves of PCSs electrodes at 1.0 A $g^{-1}$ (b), capacitances *vs* current densities of the carbon-based electrodes (c), and Nyquist plots of PCSs electrodes (d) in 6 M KOH electrolyte.

**Table S3. Electrochemical performance of carbon based KOH-electrolyte symmetric supercapacitors.**

| Materials | Current Density ($A g^{-1}$) | Device Capacitance ($F g^{-1}$) | Energy Density ($Wh kg^{-1}$) | Power Density ($W kg^{-1}$) | Ref. |
|---|---|---|---|---|---|
| ZTC-P300 | 1.25 | 216 | 7.5 | 625 | 1 |
| 800AC | 0.3 | 105 | 3.0 | 220 | 2 |
| PNC-900 | 0.1 | 236 | 8.2 | 250 | 3 |
| NOCS-1/10 | 0.5 | 130 | 4.3 | 250 | 4 |
| a-CNS/EG-10 | 0.3 | 210 | 7.3 | 500 | 5 |
| ACG-200 | 1.0 | 162 | 7.5 | 200 | 6 |
| 200-HTC-800-3 | 0.4 | 239 | 8.11 | 400 | 7 |
| N-OMCN@GN | 1 | 242.3 | 6.68 | 250 | 8 |
| MOLC | 0.5 | 211 | 3.85 | 27.7 | 9 |
| CDC | 1 | 173 | – | – | 10 |
| a-CA | 0.5 | 198.4 | 6.85 | 400 | 11 |
| CNT | 1 | 7.7 | – | – | 12 |
| $PCS_{800}$ | 0.5 | 267 | 9.23 | 400 | This work |

**Table S4. Electrochemical performance of carbon based $Na_2SO_4$-electrolyte symmetric supercapacitors.**

| Materials | Current Density (A g$^{-1}$) | Device Capacitance (F g$^{-1}$) | Energy Density (Wh kg$^{-1}$) | Power Density (W kg$^{-1}$) |
|---|---|---|---|---|
| PCF-700 | 0.5 | 32 | 13.9 | 460 |
| WJC-800 | 0.5 | 44 | 18.6 | 400 |
| G/CNTs-200 | 0.2 | 33 | 8 | 900 |
| $IPC_{2\text{-}0.2\text{-}8}$ | 0.5 | 50 | 21.9 | 461 |
| BNDC | 0.2 | 45 | 22.7 | 200 |
| HPCs | 0.5 | 30 | 14.2 | 444.5 |
| PCACM | 0.5 | 44.5 | 10.42 | 8928 |
| $PCS_{800}$ | 0.5 | 74.2 | 33.37 | 450 |

**Reference**

(1) Teng, C.; Han, Y.; Fu, G.; Hu, J.; Zheng, H.; Lu, X.; Jiang, J., Isostatic Pressure-Assisted Nanocasting Preparation of Zeolite Templated Carbon for High-Performance and Ultrahigh Rate Capability Supercapacitors. *J. Mater. Chem. A* **2018,** *6*, 18938−18947.

(2) Liu, W.; Zhang, S.; Dar, S. U.; Zhao, Y.; Akram, R.; Zhang, X.; Jin, S.; Wu, Z.; Wu, D., Polyphosphazene-Derived Heteroatoms-Doped Carbon Materials for Supercapacitor Electrodes. *Carbon* **2018,** *129*, 420−427.

(3) Zhu, G.; Ma, L.; Lv, H.; Hu, Y.; Chen, T.; Chen, R.; Liang, J.; Wang, X.; Wang, Y.; Yan, C., Pine Needle-Derived Microporous Nitrogen-Doped Carbon Frameworks Exhibit High Performances in Electrocatalytic Hydrogen Evolution Reaction and Supercapacitors. *Nanoscale* **2017,** *9*, 1237–1243.

(4) Zhang, R.; Jing, X.; Chu, Y.; Wang, L.; Kang, W.; Wei, D.; Li, H.; Xiong, S., Nitrogen/Oxygen Co-Doped Monolithic Carbon Electrodes Derived From Melamine Foam for High-Performance Supercapacitors. *J. Mater. Chem. A* **2018,** *6*, 17730–17739.

(5) Liu, Y.; Qiu, X.; Liu, X.; Liu, Y.; Fan, L. Z., 3D Porous Binary-Heteroatom Doped Carbon Nanosheet/Electrochemically Exfoliated Graphene Hybrids for High Performance Flexible Solid-State Supercapacitors. *J. Mater. Chem. A* **2018,** *6*, 8750−8756.

(6) Chen, Z.; Liu, K.; Liu, S.; Xia, L.; Fu, J.; Zhang, X.; Zhang, C.; Gao, B., Porous Active Carbon Layer Modified Graphene for High-Performance Supercapacitor. *Electrochim. Acta* **2017,** *237*, 102−108.

(7) Wu, Y.; Cao, J.; Zhao, X.; Hao, Z.; Zhuang, Q.; Zhu, J.; Wang, X.; Wei, X., Preparation of Porous Carbons by Hydrothermal Carbonization and KOH Activation of Lignite and Their Performance for Electric Double Layer Capacitor. *Electrochim. Acta* **2017,** *252*, 397−407.

(8) Zhao, M.; Cui, X.; Chen, L.; Xu, Y.; He, Z.; Yang, S.; Yi, W., Ordered Mesoporous Carbon Nanosphere-Encapsulated Graphene Network with Optimized Nitrogen Doping for Enhanced Supercapacitor Performance. *Nanoscale* **2018**, *10*, 15379–15386.

(9) Shaibani, M.; Smith, S. J. D.; Banerjee, P. C.; Konstas, K.; Zafari, A.; Lobo, D. E.; Nazari, M.; Hollenkamp, A. F.; Hill, M. R.; Majumder, M., Framework-Mediated Synthesis of Highly Microporous Onion-Like Carbon: Energy Enhancement in Supercapacitors without Compromising Power. *J. Mater. Chem.* A **2017**, *5*, 2519−2529.

(10) Yair, K.; Marcus, R.; Emanuel, K.; Lars, B.; Alexander, K.; Stefan, K.; Gleb, Y., High-Rate Electrochemical Capacitors Based on Ordered Mesoporous Silicon Carbide-Derived Carbon. *ACS Nano* **2010**, *4*, 1337−1344.

(11) Zhang, Y.; Zhao, C.; Ong, W. K.; Lu, X., Ultrafast-Freezing-Assisted Mild Preparation of Biomass-Derived, Hierarchically Porous, Activated Carbon Aerogels for High-Performance Supercapacitors. *ACS Sustain. Chem. Eng.* **2018**, *7*, 403−411.

(12) Pan, S.; Lin, H.; Deng, J.; Chen, P.; Chen, X.; Yang, Z.; Peng, H., Novel Wearable Energy Devices Based on Aligned Carbon Nanotube Fiber Textiles. *Adv. Energy Mater.* **2015**, *5*, 1401438.